

Finite-temperature theory of amorphous magnetic alloys

M. Yu and Y. Takehashi

Hokkaido Institute of Technology, Maeda, Teine-ku, Sapporo 006, Japan

H. Tanaka

IBM Research, Tokyo Research Laboratory, IBM Japan Ltd. 1623-14, Shimotsuruma, Yamato, Kanagawa 242, Japan

(Received 28 June 1993)

A finite-temperature theory of magnetism in amorphous magnetic alloys with strong environment effects is developed on the basis of the functional integral method for thermal spin fluctuations and the distribution-function method for random distribution of local magnetic moments. The theory drastically simplifies numerical calculations by means of the geometrical-mean model for amorphous structure as well as electronic structure, and allows us to investigate the magnetism in amorphous transition-metal alloys with large difference in atomic size via average coordination number which depends on the type of central atom. Numerical example is given of the amorphous Fe-Zr alloys. It is demonstrated that the theory reproduces quantitatively the local densities of states obtained from the first-principles calculations, and describes the magnetic phase diagram, in particular, the itinerant-electron spin glass. It is also shown that the atomic-size effects play an important role in the formation of ferromagnetism in concentrated Fe-Zr amorphous alloys. The reentrant spin-glass behavior around 90 at. % Fe is shown to be due to the thermal spin fluctuations of amplitudes of local magnetic moments.

I. INTRODUCTION

Finite-temperature theories which allow us to investigate the magnetic properties of a large number of amorphous transition-metal (TM) alloys have become indispensable with the appearance of intriguing experimental data for early-TM TM amorphous alloys, and rare-earth TM amorphous alloys,¹⁻⁸ which cannot be explained by a simple concept such as the charge transfer or the generalized Slater-Pauling curves.⁹⁻¹² For example, the amorphous Fe-Zr alloys show complex magnetism: paramagnetism (P), ferromagnetism (F), and spin glass (SG) with increasing Fe concentration.^{4,5} The magnetization vs concentration curve deviates from the generalized Slater-Pauling curves beyond 85 at. % Fe.^{5,13-15} Neither the concentration dependence of SG temperatures (T_g) nor that of Curie temperatures (T_C) has been explained. The reentrant spin-glass (RSG) behavior near the SG-F boundary has not been clarified yet, though much experimental effort has been concentrated on this issue in the past decade.³⁻⁶

A single-site theory of finite-temperature magnetism in amorphous and liquid alloys was first proposed by one of the authors¹⁶ on the basis of the functional integral method¹⁷⁻¹⁹ and the coherent potential approximation.^{16,19,20} The theory explained the qualitative behaviors of high-temperature susceptibilities in liquid Fe, Co, and Ni and clarified the importance of thermal spin fluctuations in the liquid data. The applications to amorphous and liquid alloys, however, were not easy since one needs to calculate there the input averaged densities of states (DOS) for noninteracting electrons at each concentration. Yu and Takehashi²¹ solved this difficulty combining the single-site theory with the geometrical-mean (GM) model^{22,23} for both interatomic distances and

transfer integrals. The approach enables us to calculate the magnetic properties at arbitrary concentration only from the electronic structures of amorphous pure metals. It was applied to the amorphous Fe-Ni alloys and explained the enhancement of ferromagnetism in the Invar concentration region.²⁴

A theory which takes into account local environment effects (LEE's), therefore describes the SG in amorphous metals and alloys, was proposed by Takehashi.²⁵ He investigated systematically various magnetic properties of amorphous 3d TM's using the theory,^{26,27} and provided us with a picture of metallic magnetism in amorphous TM's: the formation of the SG around Fe, the enhancement of T_C around Co, and the weak ferromagnetism around Ni. This theory, however, leaves two problems unsolved when amorphous alloys are considered. First, it neglects the atomic-size effects on coordination number which may play an important role in early-TM TM and rare-earth TM amorphous alloys. Second, it does not give us any method to calculate the input average DOS for amorphous alloys, which are indispensable for the actual numerical calculations.

In this article, we present an improved theory which takes into account the atomic-size effects by introducing an average coordination number z_α^* depending on the type of central atom α , and greatly simplifies numerical calculations with use of the GM model.^{22,23} This theory enables us to study various magnetic properties of 3d-3d as well as 3d-4d and 3d-5d amorphous TM alloys at arbitrary concentration. In particular, the present theory describes not only the itinerant-electron SG, in which amplitude fluctuations of spins play an important role, but also the effects of atomic short-range order (ASRO) on magnetism.

We will describe the theoretical framework in detail in

the following section, which consists of four parts. In Sec. II A, we transform the degenerate-bands Hubbard model into a noninteracting electron system with fictitious random exchange fields, using the functional integral method.¹⁷⁻¹⁹ A local magnetic moment (LM) is then given by a classical average of the fictitious field variable on the same site with respect to the energy functional. In Sec. II B, we treat the electronic structure of amorphous alloys in the energy functional by means of a Bethe-type approximation and the GM model outside a cluster. In the present approach, the coordination number is treated as a random variable so that z_α^* is introduced as a new parameter. Next, we take into account the LEE's on the central LM in Sec. II C, using the distribution-function method initiated by Matsubara²⁸ and Katsura *et al.*²⁹ The self-consistent equations for the average LM and the SG order parameter are derived there. In Sec. II D, we discuss the choice of parameters which are needed in the actual calculations. In particular, we will give a simple expression for the average coordination number z_α^* as well as a condition of the most random atomic configuration with respect to the ASRO parameters.

We will present some results for the amorphous Fe-Zr alloys in Sec. III as a numerical example. We will demonstrate that the theory reproduces the local DOS obtained from the first-principles calculations³⁰ quantitatively and the magnetic phase diagram qualitatively or semiquantitatively. The mechanism for the formations of the SG, RSG, and ferromagnetism is presented there. Finally, in Sec. IV, we will summarize our results, and discuss future developments of the theory.

II. FINITE-TEMPERATURE THEORY WITH LOCAL ENVIRONMENT EFFECTS

A. Functional integral method

We consider binary amorphous alloys described by the degenerate-band Hubbard model with Hund's rule coupling, and adopt the functional integral method¹⁷⁻¹⁹ to take into account thermal spin fluctuations. The interacting electron system is then transformed into a one-electron system with time-dependent fictitious fields $\{\xi_i(\tau)\}$ acting on each site i . Within the static approximation,³¹ in which the time dependence of the fictitious field variables is neglected [i.e., $\xi_i(\tau) = \xi_i$, being static in time], the thermal average of LM on the site 0 is given by a classical average of the field variable on the same site as follows:^{32,33}

$$\langle m_0 \rangle = \frac{\int \left[\prod_{i=0}^{N-1} d\xi_i \right] \xi_0 e^{-\beta E(\xi)}}{\int \left[\prod_{i=0}^{N-1} d\xi_i \right] e^{-\beta E(\xi)}}. \quad (1)$$

Here β is the inverse temperature.

The energy $E(\xi)$ in Eq. (1) consists of the one-electron free energy with random exchange fields $\{\xi_i\}$, the term with charge potentials $\{w_i(\xi)\}$ leading to a given d electron number n_i on site i , and the Gaussian term describ-

ing random exchange fields:

$$E(\xi) = \int d\omega f(\omega) \frac{D}{\pi} \text{Im tr}[\ln(L'^{-1} - t')] + \sum_i [-n_i w_i(\xi) + \frac{1}{4} \bar{J}_i \xi_i^2]. \quad (2)$$

Here we have adopted the D -fold equivalent-bands model for brevity, and have neglected the transverse-field variables which cause unreasonable thermodynamics within the static approximation.³² $f(\omega)$ in Eq. (2) denotes the Fermi distribution function and \bar{J}_i the effective exchange energy parameter on site i . The locator matrix L' for σ -spin electrons is defined by

$$(L'^{-1})_{ij\sigma} \equiv [\omega + i\delta - \epsilon_i + \mu - w_i(\xi) + \frac{1}{2} \bar{J}_i \xi_i \sigma + h\sigma] \delta_{ij}. \quad (3)$$

Here δ is an infinitesimal positive number, ϵ_i and μ are the atomic level and the chemical potential, respectively. h denotes the external field. The matrix $(t')_{ij}$ is defined by the transfer integral between sites i and j as follows:

$$(t')_{ij} \equiv t'(R_{ij}), \quad (4)$$

where R_{ij} is the interatomic distance between the sites i and j .

In the amorphous magnetic alloys, the structural and configurational disorders appear in both the diagonal matrix L' and the off-diagonal matrix t' . This makes it very difficult to treat the first term in Eq. (2). We therefore simplify the transfer integral $t'(R_{ij})$ between the types of atoms α and γ by means of a geometrical mean,²³

$$t'(R_{ij}) = t^{\alpha\gamma}(R_{ij}) = [t^{\alpha\alpha}(R_{ij}) t^{\gamma\gamma}(R_{ij})]^{1/2}, \quad (5)$$

which is recognized as a reasonable approximation in TM alloys.³⁴ Assuming that the transfer integral follows the same power law with respect to the interatomic distance^{35,36}

$$t'(R_{ij}) \propto R_{ij}^{-\kappa}, \quad (6)$$

κ being independent of the type of atom, we obtain the following relation:

$$t'(R_{ij}) = r_\alpha^{*(c)} t(R_{ij}) r_\gamma^{(c)}. \quad (7)$$

Here $t(R_{ij})$ can be chosen as $t^{\text{BB}}(R_{ij})$ so that the factor $r_\alpha^{(c)}$ only depends on the type of atom α

$$r_\alpha^{(c)} = \left[\frac{t^{\alpha\alpha}(R_{ij})}{t^{\text{BB}}(R_{ij})} \right]^{1/2}. \quad (8)$$

It should be noted that $t(R_{ij}) = t^{\text{BB}}(R_{ij})$ still depends on the types of atoms α and γ via $R_{ij} = R_{ij}^{\alpha\gamma}$.

The energy function $E(\xi)$ is then rewritten as

$$E(\xi) = \int d\omega f(\omega) \frac{D}{\pi} \text{Im tr}[\ln(L^{-1} - t)] + \sum_i [-n_i w_i(\xi) + \frac{1}{4} \bar{J}_i \xi_i^2]. \quad (9)$$

Here $(L)_{ij\sigma} = L_{i\sigma} \delta_{ij}$ is a renormalized locator matrix

defined by

$$L_{i\sigma}^{-1} = |r_\alpha^{(c)}|^{-2} \mathcal{L}'_{i\sigma}{}^{-1}, \quad (10)$$

and t is the transfer integral matrix defined by

$$(t)_{ij} \equiv t(R_{ij}). \quad (11)$$

Next, we introduce a site-dependent effective medium $\{\mathcal{L}'_{i\sigma}\}$ to describe the effects of random potentials and thermal spin fluctuations in the diagonal matrix L as an average, and expand the scattering potential $(L^{-1} - \mathcal{L}'^{-1})$ in Eq. (9) with respect to the site:

$$E(\xi) = \sum_i E_i(\xi_i) + \sum_{(ij)} \Phi_{ij}(\xi_i, \xi_j) + \cdots. \quad (12)$$

The zeroth-order term in Eq. (12) has been omitted, since it is described by the effective medium only. Thus, the energy $E(\xi)$ consists of the sum of a single-site energy functional $E_i(\xi_i)$ on each site:

$$E_i(\xi_i) = \int d\omega f(\omega) \frac{D}{\pi} \text{Im} \sum_\sigma \ln(L_{i\sigma}^{-1} - \mathcal{L}'_{i\sigma}{}^{-1} + F'_{ii\sigma}{}^{-1}) - n_i w_i(\xi) + \frac{1}{4} \tilde{J}_i \xi_i^2, \quad (13)$$

the sum of pair energy $\Phi_{ij}(\xi_i, \xi_j)$:

$$\begin{aligned} & \Phi_{ij}(\xi_i, \xi_j) \\ &= \int d\omega f(\omega) \frac{D}{\pi} \text{Im} \sum_\sigma \ln[1 - \tilde{t}'_{i\sigma}(\xi_i) \tilde{t}'_{j\sigma}(\xi_j) F'_{ij\sigma} F'_{ji\sigma}], \end{aligned} \quad (14)$$

and the higher-order terms. $F'_{ii\sigma}$ ($F'_{ij\sigma}$) in Eq. (13) [Eq. (14)] is the diagonal (off-diagonal) term of coherent Green's function defined by

$$F'_{ij\sigma} = [(\mathcal{L}'^{-1} - t)^{-1}]_{ij\sigma}, \quad (15)$$

and $\tilde{t}'_{i\sigma}(\xi_i)$ is the single-site t matrix defined by

$$\tilde{t}'_{i\sigma}(\xi_i) = \frac{L_{i\sigma}^{-1} - \mathcal{L}'_{i\sigma}{}^{-1}}{1 + (L_{i\sigma}^{-1} - \mathcal{L}'_{i\sigma}{}^{-1}) F'_{ii\sigma}}. \quad (16)$$

The effective medium $\mathcal{L}'_{i\sigma}$ is chosen so that the higher-order correction in Eq. (12) becomes as small as possible. This leads to a condition that the average single-site t matrix vanishes on each site:

$$[[\langle \tilde{t}'_{i\sigma}(\xi_i) \rangle]_s]_c = 0. \quad (17)$$

Here $\langle \rangle$ denotes the thermal average, and $[]_s$ ($[]_c$) denotes the structural (configurational) average. Equation (17) is called the CPA (coherent potential approximation) equation.^{16,19,20} The charge potential w_i in Eqs. (13) and (16) is determined from the charge-neutrality condition

$$n_i = \int d\omega f(\omega) \frac{-D}{\pi} \text{Im} \sum_\sigma \frac{1}{|r_\alpha^{(c)}|^2} (L_{i\sigma}^{-1} - \mathcal{L}'_{i\sigma}{}^{-1} + F'_{ii\sigma}{}^{-1})^{-1}. \quad (18)$$

In the following, we neglect the higher-order term, and only take into account the nearest-neighbor (NN) pair en-

ergies in Eq. (12) because of the strong damping of interaction strength in the disordered system as a function of interatomic distance.³⁷ After making use of a decoupling approximation to the surrounding field variables in Eq. (1), which is correct up to the second moment, and a molecular-field approximation in the thermal average of LM on site 0,²⁵ we obtain

$$\langle m_0 \rangle = \frac{\int d\xi \xi e^{-\beta\Psi(\xi)}}{\int d\xi e^{-\beta\Psi(\xi)}}, \quad (19)$$

$$\Psi(\xi) = E_0(\xi) + \sum_{j \neq 0} \Phi_{0j}^{(a)}(\xi) - \sum_{j \neq 0} \Phi_{0j}^{(e)}(\xi) \frac{\langle m_j \rangle}{x_j}. \quad (20)$$

Here $E_0(\xi)$ in Eq. (20) is the single-site energy functional on site 0 [see Eq. (13)], and $\Phi_{ij}^{(a)}(\xi)$ and $\Phi_{ij}^{(e)}(\xi)$ are the atomic and the exchange pair energies defined by

$$\begin{bmatrix} \Phi_{ij}^{(a)}(\xi) \\ \Phi_{ij}^{(e)}(\xi) \end{bmatrix} = \frac{1}{2} \sum_{\nu=\pm} \begin{bmatrix} 1 \\ -\nu \end{bmatrix} \Phi_{ij}(\xi, \nu x_j). \quad (21)$$

The amplitude x_j in Eqs. (20) and (21) is defined by

$$x_j^2 = \frac{\int d\xi \xi^2 e^{-\beta E_j(\xi)}}{\int d\xi e^{-\beta E_j(\xi)}}, \quad (22)$$

and is approximated by its average value $[x_{\gamma_j}]_s$ in the following, where γ_j denotes the type of atom on site j . The formulation until here is essentially the same as in that of substitutional alloys. (See Ref. [38] for more details.)

B. Calculation of coherent Green's functions

A simplified method calculating the coherent Green's functions $F'_{ij\sigma}$ with structural disorder in Eqs. (13) and (14) has recently been proposed in our paper.²³ Let us consider a cluster which consists of the central atom α and neighboring atoms on its NN shell. We then expand the coherent Green's functions with respect to the locator $\{\mathcal{L}'_{i\sigma}\}$ as follows:³⁹

$$F'_{00\sigma} = \mathcal{L}'_{0\sigma} + \mathcal{L}'_{0\sigma} \sum_{j \neq 0}^z t_{0j} F'_{j0\sigma}, \quad (23)$$

$$\begin{aligned} F'_{j0\sigma} &= \mathcal{L}'_{j\sigma} t_{j0} F'_{00\sigma} + \mathcal{L}'_{j\sigma} S'_{j\sigma}(\mathcal{L}'_{j\sigma}) F'_{j0\sigma} \\ &+ \sum_{i \neq j, 0} T'_{ji}(\mathcal{L}'_{i\sigma}) F'_{i0\sigma}. \end{aligned} \quad (24)$$

The self-energy $S'_{j\sigma}$ (T'_{ji}) denotes the sum of all the paths, which start from site j and end at site j (i) without returning to the cluster on the ways.

After adopting the Bethe approximation [i.e., $T'_{ji} \approx 0$ in Eq. (24)], we obtain

$$F'_{00\sigma} = \left[\mathcal{L}'_{0\sigma}{}^{-1} - \sum_{j \neq 0}^z \frac{t_{0j}^2}{\mathcal{L}'_{j\sigma}{}^{-1} - S'_{j\sigma}(\mathcal{L}'_{j\sigma})} \right]^{-1}, \quad (25)$$

$$F'_{0j\sigma} = F'_{j0\sigma} = \frac{t_{0j}}{\mathcal{L}'_{j\sigma}{}^{-1} - S'_{j\sigma}(\mathcal{L}'_{j\sigma})} F'_{00\sigma}. \quad (26)$$

Here we can treat the coordination number z of the cen-

tral atom as a random variable in Eq. (25). Note that it was regarded as a constant previously.²⁵⁻²⁷

Next, we treat the interatomic distance $R_{0j}^{\alpha\gamma}$ between the central atom α and the neighboring atom γ on the NN shell by means of the GM model:^{22,23}

$$R_{0j}^{\alpha\gamma} = (R_{0j}^{\alpha\alpha} R_{0j}^{\gamma\gamma})^{1/2}. \quad (27)$$

This relation holds true within a few percent errors as we emphasized in a previous paper.²³ The transfer integral $t_{0j}(R_{0j}) = t(R_{0j}^{\alpha\gamma})$ is then written as

$$t(R_{0j}^{\alpha\gamma}) = r_{\alpha}^{*(s)} \hat{t}_{0j} r_{\gamma}^{(s)}, \quad (28)$$

where the factor $r_{\alpha}^{(s)}$ is given by

$$r_{\alpha}^{(s)} = \left[\frac{t(R_{0j}^{\alpha\alpha})}{t(R_{0j}^{\text{BB}})} \right]^{1/2}. \quad (29)$$

At this stage, $\hat{t}_{0j} \equiv t^{\text{BB}}(R_{0j}^{\text{BB}})$ does not depend on the atomic configuration any more. The coherent Green's function $F'_{00\sigma}$ is then expressed with use of the renormalized locator $\mathcal{L}_{j\sigma} \equiv |r_j^{(s)}|^2 \mathcal{L}'_{j\sigma}$ as follows:

$$F'_{00\sigma} = \frac{1}{|r_{\alpha}^{(s)}|^2} \left[\mathcal{L}_{0\sigma}^{-1} - \sum_{j \neq 0}^z \frac{\hat{t}_{0j}^2}{\mathcal{L}_{j\sigma}^{-1} - S'_{j\sigma} / |r_j^{(s)}|^2} \right]^{-1}. \quad (30)$$

Since the self-energy $S'_{j\sigma}$ in Eq. (30) contains all the structural disorder outside the cluster, it brings us the difficulties in the calculation of $F'_{00\sigma}$. To simplify it, we make further approximations. First, we choose the effective medium $\mathcal{L}_{j\sigma}$ to be site-independent in the following ($\mathcal{L}_{j\sigma} = \mathcal{L}_{\sigma}$). Second, we adopt the GM model outside the cluster. This model, in addition to Eqs. (5) and (6), assumes (i) $R_{ij}^{\alpha\gamma} = (R_{ij}^{\alpha\alpha} R_{ij}^{\gamma\gamma})^{1/2}$ for any interatomic distance, and (ii) similarity in structures between amorphous pure metals A and B . We have shown in a previous paper²³ that this model leads to a good description of electronic structure outside the cluster. Then, Eq. (30) can be written as

$$F'_{00\sigma} = |r_{\alpha}^{(s)}|^{-2} F_{00\sigma}, \quad (31)$$

$$F_{00\sigma} = \left[\mathcal{L}_{\sigma}^{-1} - \sum_{j \neq 0}^z \frac{\hat{t}_{0j}^2}{\mathcal{L}_{\sigma}^{-1} - S_{j\sigma}(\mathcal{L}_{\sigma})} \right]^{-1}. \quad (32)$$

Here $S_{j\sigma}(\mathcal{L}_{\sigma}) \equiv |r_j^{(s)}|^2 S'_{j\sigma}(\mathcal{L}_{\sigma})$ is the renormalized self-energy in the GM model.

In the same way, we approximate the coherent Green's functions $F'_{j0\sigma}$ in Eq. (26) and $F'_{jj\sigma}$ as follows:

$$F'_{j0\sigma} = (r_j^{*(s)} r_0^{(s)})^{-1} F_{j0\sigma}, \quad (33)$$

$$F_{j0\sigma} = \frac{\hat{t}_{0j}}{\mathcal{L}_{\sigma}^{-1} - S_{j\sigma}(\mathcal{L}_{\sigma})} F_{00\sigma}, \quad (34)$$

$$F'_{jj\sigma} = |r_j^{(s)}|^{-2} F_{jj\sigma}, \quad (35)$$

$$F_{jj\sigma} = (\mathcal{L}_{\sigma}^{-1} - \hat{t})^{-1}. \quad (36)$$

Substituting Eqs. (31)–(36) into Eqs. (13), (14), and (18), we obtain

$$E_0(\xi) = \int d\omega f(\omega) \frac{D}{\pi} \text{Im} \sum_{\sigma} \ln(\hat{\mathcal{L}}_{0\sigma}^{-1} - \mathcal{L}_{\sigma}^{-1} + F_{00\sigma}^{-1}) + n_0 w_0(\xi) + \frac{1}{4} \bar{J}_0 \xi^2, \quad (37)$$

$$E_j(\xi) = \int d\omega f(\omega) \frac{D}{\pi} \text{Im} \sum_{\sigma} \ln(\hat{\mathcal{L}}_{j\sigma}^{-1} - \mathcal{L}_{\sigma}^{-1} + F_{jj\sigma}^{-1}) - n_j w_j(\xi) + \frac{1}{4} \bar{J}_j \xi^2, \quad (38)$$

$$\Phi_{0j}(\xi, \xi_j) = \int d\omega f(\omega) \frac{D}{\pi} \text{Im} \sum_{\sigma} \ln[1 - \tilde{t}_{0\sigma}(\xi) \tilde{t}_{j\sigma}(\xi_j) F_{0j\sigma} F_{j0\sigma}], \quad (39)$$

$$n_i = \int d\omega f(\omega) \frac{-D}{\pi} \text{Im} \sum_{\sigma} \frac{1}{|r_i|^2} (\hat{\mathcal{L}}_{i\sigma}^{-1} - \mathcal{L}_{\sigma}^{-1} + F_{ii\sigma}^{-1})^{-1}. \quad (40)$$

Here the renormalized locator $\hat{\mathcal{L}}_{i\sigma}$ ($i=0, j$) is defined by

$$\hat{\mathcal{L}}_{i\sigma} = |r_i|^2 \mathcal{L}'_{i\sigma}, \quad (41)$$

$$|r_i|^2 = |r_i^{(s)}|^2 |r_i^{(c)}|^2, \quad (42)$$

and the single-site t matrix $\tilde{t}'_{i\sigma}(\xi_i)$ [Eq. (16)] reduces to $\tilde{t}_{i\sigma}(\xi_i)$ defined by

$$\tilde{t}_{i\sigma}(\xi_i) = \frac{\hat{\mathcal{L}}_{i\sigma}^{-1} - \mathcal{L}_{\sigma}^{-1}}{1 + (\hat{\mathcal{L}}_{i\sigma}^{-1} - \mathcal{L}_{\sigma}^{-1}) F_{ii\sigma}}. \quad (43)$$

The CPA equation reduces to

$$[[\langle \hat{\mathcal{L}}_{i\sigma}(\xi_i) \rangle]_s]_c = 0. \quad (44)$$

These equations are explicitly influenced by the structural disorder outside the cluster via $S_{j\sigma}(\mathcal{L}_{\sigma})$ and $F_{jj\sigma}$. When we take a structural average outside the cluster, we replace $S_{j\sigma}(\mathcal{L}_{\sigma})$ with the effective self-energy \mathcal{S}_{σ} and $F_{jj\sigma}$ with its structural average $[F_{jj\sigma}]_s$. The coherent Green's functions are then expressed as

$$F_{00\sigma} = \left[\mathcal{L}_{\sigma}^{-1} - \sum_{j \neq 0}^z \hat{t}_{0j}^2 \mathcal{H}_{\sigma} \right]^{-1}, \quad (45)$$

$$F_{j0\sigma} = t_{0j} \mathcal{H}_{\sigma} F_{00\sigma}, \quad (46)$$

$$[F_{jj\sigma}]_s = F_{\sigma} = \int \frac{[\rho(\epsilon)]_s d\epsilon}{\mathcal{L}_{\sigma} - \epsilon}. \quad (47)$$

Here

$$\mathcal{H}_{\sigma} = (\mathcal{L}_{\sigma}^{-1} - \mathcal{S}_{\sigma})^{-1}. \quad (48)$$

The effective self-energy \mathcal{S}_{σ} is determined so that the structural average of the diagonal Green's function [Eq. (45)] recovers the exact form:

$$\left[\left[\mathcal{L}_{\sigma}^{-1} - \sum_{j \neq 0}^z \hat{t}_{0j}^2 \mathcal{H}_{\sigma} \right]^{-1} \right]_s = F_{\sigma}. \quad (49)$$

A simplified expression for Eq. (49) has been obtained in a previous work²³ by adopting a decoupling approximation to a random variable $\theta = \sum_j \hat{t}_{j0}^2$:

$$\frac{1}{2} \sum_{\nu=\pm} \left[\mathcal{L}_{\sigma}^{-1} - \left[1 + \nu \frac{[(\delta\theta)^2]_s^{1/2}}{[\theta]_s} \right] [\theta]_s \mathcal{H}_{\sigma} \right]^{-1} = F_{\sigma}. \quad (50)$$

Solving this equation, we obtain

$$[\theta]_s \mathcal{H}_\sigma = \frac{2F_\sigma \mathcal{L}_\sigma^{-1} - 1 \pm \{1 + 4([\delta\theta]^2)_s / [\theta]_s^2\} F_\sigma \mathcal{L}_\sigma^{-1} (F_\sigma \mathcal{L}_\sigma^{-1} - 1)^{1/2}}{2\{1 - ([\delta\theta]^2)_s / [\theta]_s^2\} F_\sigma} . \quad (51)$$

The sign at the right-hand side of Eq. (51) should be taken so that $\text{Im}[\theta]_s \mathcal{H}_\sigma < 0$.

The average DOS $[\rho(\epsilon)]_s$ in F_σ [see Eq. (47)] depends on concentration in the case of the $3d-4d$ and $3d-5d$ amorphous TM alloys since the shapes of the DOS for constituent elements are considerably different from each other. In this case, we take into account the concentration dependence with use of a common band model

$$\hat{t}_{ij} = \lambda \hat{t}_{ij} = \lambda [c_A t_{ij}(A) + c_B t_{ij}(B)] . \quad (52)$$

Here λ is a normalization factor and $t_{ij}(\alpha) \equiv t^{\alpha\alpha}(R_{ij}^{\alpha\alpha}, c_\alpha = 1)$.

Approximate expression for \mathcal{H}_σ has been obtained in our recent work [see Eq. (60) in Ref. 23]

$$\mathcal{H}_\sigma = (c_A \mathcal{H}_{A\sigma}^{-1} + c_B \mathcal{H}_{B\sigma}^{-1})^{-1} , \quad (53)$$

$$\mathcal{H}_{\alpha\sigma} = \frac{2F_{\alpha\sigma} \mathcal{L}_\sigma^{-1} - 1 \pm \{1 + 4([\delta\theta]^2)_s / [\theta]_s^2\} F_{\alpha\sigma} \mathcal{L}_\sigma^{-1} (F_{\alpha\sigma} \mathcal{L}_\sigma^{-1} - 1)^{1/2}}{2\lambda^2 \mu_2(\alpha) \{1 - ([\delta\theta]^2)_s / [\theta]_s^2\} F_{\alpha\sigma}} , \quad (54)$$

$$F_{\alpha\sigma} = \int \frac{[\rho_\alpha(\epsilon)]_s d\epsilon}{\mathcal{L}_\sigma - \lambda\epsilon} , \quad (55)$$

$$\lambda = \frac{\mu_2(B)^{1/2}}{c_A \mu_2(A)^{1/2} + c_B \mu_2(B)^{1/2}} . \quad (56)$$

Here $[\rho_\alpha(\epsilon)]_s$ denotes the average DOS for noninteracting electrons in amorphous pure metal α . $\mu_2(\alpha)$ is the second moment for the averaged DOS,

$$\mu_2(\alpha) = \int (\epsilon - \epsilon_\alpha)^2 [\rho_\alpha(\epsilon)]_s d\epsilon . \quad (57)$$

C. Distribution-function method

After having introduced the effective medium \mathcal{L}_σ and the effective self-energy \mathcal{S}_σ , the central LM in Eq. (19) is regarded as a function of the surrounding LM's $\{\langle m_j \rangle\}$ on the NN shell, the squares of transfer integrals $\{y_j = \hat{t}_{j0}^2\}$, the atomic configuration on the NN shell $\{\gamma_j\}$, and the coordination number z . These variables randomly change because of the structural and configurational disorders. We therefore introduce a probability $g_{\gamma_j}(m_j) dm_j$ of finding LM on the atom of type γ_j between m_j and $m_j + dm_j$, a probability $p_s(y_j) dy_j$ of finding the square of the transfer integral between y_j and $y_j + dy_j$, a probability $p_z^{\alpha\alpha}$ of finding an atom of type α at the neighboring site of the central atom α when z is given, and a probability $p_\alpha(z)$ of finding z sites on the NN shell of the central atom α . These distribution functions determine the distribution of the central LM via Eq. (19) and the latter should be identical with those at the neighboring sites. We therefore obtain an integral equation for the distribution of LM's in the same way as in a previous paper:²⁵

$$g_\alpha(M) = \sum_z p_\alpha(z) \sum_{n=0}^z \Gamma(n, z, p_z^{\alpha\alpha}) \int \delta(M - \langle m_\alpha \rangle) \prod_{i=1}^n [p_s(y_i) dy_i g_\alpha(m_i) dm_i] \prod_{j=n+1}^z [p_s(y_j) dy_j g_{\bar{\alpha}}(m_j) dm_j] . \quad (58)$$

Here the atomic configuration is described by a binomial distribution function with the coordination number z and the number of α atom n on the NN shell:

$$\Gamma(n, z, p^{\alpha\alpha}) = \frac{z!}{n!(z-n)!} (p^{\alpha\alpha})^n (1 - p^{\alpha\alpha})^{z-n} , \quad (59)$$

since we have adopted the Bethe-type approximation to the surrounding sites and have neglected the z dependence of $p_z^{\alpha\alpha}$ for brevity. The latter is written by Cowley's ASRO parameter τ_α as follows:

$$p^{\alpha\alpha} = c_\alpha + (1 - c_\alpha) \tau_\alpha . \quad (60)$$

A new feature in the integral Eq. (58) is that the distribution of the coordination number $[p_\alpha(z)]$ is taken into account. We adopt here a simple form for the distribution function

$$p_\alpha(z) = (z_\alpha^* - [z_\alpha^*]) \delta_{z[z_\alpha^*]+1} + ([z_\alpha^*] + 1 - z_\alpha^*) \delta_{z[z_\alpha^*]} . \quad (61)$$

This describes the average coordination number $z_\alpha^* = \sum_z p_\alpha(z) z$, but does not necessarily describe the fluctuations around z_α^* .

We further simplify the 2z-fold integrals in Eq. (58) making use of the decoupling approximation as follows:

$$\int m^{2n+k} g_\alpha(m) dm \approx [[\langle m_\alpha \rangle]_s]_c^n [[\langle m_\alpha \rangle^k]_s]_c, \quad (62)$$

$$\int (y - [y]_s)^{2n+k} p_s(y) dy \approx [(\delta y)^2]_s^n 0^k. \quad (63)$$

These are the lowest approximations which take into account the effects of fluctuations in these distributions and have been successfully applied to the substitutional alloys.⁴⁰ Thus, the distribution function $g_\alpha(M)$ [Eq. (58)] becomes

$$g_\alpha(M) = \sum_z p_\alpha(z) \sum_{n=0}^z \Gamma(n, z, p^{\alpha\alpha}) \sum_{i=0}^n \Gamma(i, n, \frac{1}{2}) \sum_{j=0}^{z-n} \Gamma(j, z-n, \frac{1}{2}) \sum_{k_1=0}^i \Gamma(k_1, i, q_\alpha) \sum_{k_2=0}^{n-i} \Gamma(k_2, n-i, q_\alpha) \\ \times \sum_{l_1=0}^j \Gamma(l_1, j, q_{\bar{\alpha}}) \sum_{l_2=0}^{z-n-j} \Gamma(l_2, z-n-j, q_{\bar{\alpha}}) \delta[M - \langle m_\alpha \rangle(z, n, i, j, k_1, k_2, l_1, l_2)], \quad (64)$$

$$q_\alpha = \frac{1}{2} \left[1 + \frac{[[\langle m_\alpha \rangle]_s]_c}{[[\langle m_\alpha \rangle^2]_s]_c^{1/2}} \right]. \quad (65)$$

In this way, we can specify the central LM on atom α by means of the coordination number z , the number of α atoms n on the NN shell, the number i (j) of contracted atoms α ($\bar{\alpha}$) on the NN shell, the number k_1 (l_1) of fictitious spins in the up direction on the i (j) contracted atoms α ($\bar{\alpha}$), and the number k_2 (l_2) of fictitious spins in the up direction on the $n-i$ ($z-n-j$) stretched atoms α ($\bar{\alpha}$). The first and the second moments with respect to the configurational and structural disorders (i.e., $[[\langle m_\alpha \rangle]_s]_c$ and $[[\langle m_\alpha \rangle^2]_s]_c$) on the right-hand side of Eq. (64) are automatically obtained from the following self-consistent equations:

$$\left[\frac{[[\langle m_\alpha \rangle]_s]_c}{[[\langle m_\alpha \rangle^2]_s]_c} \right] = \int \left[\frac{M}{M^2} \right] g_\alpha(M) dM \\ = \sum_z p_\alpha(z) \sum_{n=0}^z \Gamma(n, z, p^{\alpha\alpha}) \sum_{i=0}^n \Gamma(i, n, \frac{1}{2}) \sum_{j=0}^{z-n} \Gamma(j, z-n, \frac{1}{2}) \sum_{k_1=0}^i \Gamma(k_1, i, q_\alpha) \\ \times \sum_{k_2=0}^{n-i} \Gamma(k_2, n-i, q_\alpha) \sum_{l_1=0}^j \Gamma(l_1, j, q_{\bar{\alpha}}) \sum_{l_2=0}^{z-n-j} \Gamma(l_2, z-n-j, q_{\bar{\alpha}}) \left[\frac{\langle \xi_\alpha \rangle(z, n, i, j, k_1, k_2, l_1, l_2)}{\langle \xi_\alpha \rangle(z, n, i, j, k_1, k_2, l_1, l_2)^2} \right]. \quad (66)$$

Here

$$\langle \xi_\alpha \rangle(z, n, i, j, k_1, k_2, l_1, l_2) = \frac{\int d\xi \xi e^{-\beta \Psi(\xi, z, n, i, j, k_1, k_2, l_1, l_2)}}{\int d\xi e^{-\beta \Psi(\xi, z, n, i, j, k_1, k_2, l_1, l_2)}}, \quad (67)$$

$$\Psi(\xi, z, n, i, j, k_1, k_2, l_1, l_2) = E_\alpha(\xi, z, i+j) + i \Phi_{\alpha\alpha+}^{(a)}(\xi, z, i+j) + (n-i) \Phi_{\alpha\alpha-}^{(a)}(\xi, z, i+j) \\ + j \Phi_{\alpha\bar{\alpha}+}^{(a)}(\xi, z, i+j) + (z-n-j) \Phi_{\alpha\bar{\alpha}-}^{(a)}(\xi, z, i+j) \\ - [(2k_1-i) \Phi_{\alpha\alpha+}^{(e)}(\xi, z, i+j) + (2k_2-n+i) \Phi_{\alpha\alpha-}^{(e)}(\xi, z, i+j)] \frac{[[\langle m_\alpha \rangle^2]_s]_c^{1/2}}{[x_\alpha]_s} \\ - [(2l_1-j) \Phi_{\alpha\bar{\alpha}+}^{(e)}(\xi, z, i+j) + (2l_2-z+n+j) \Phi_{\alpha\bar{\alpha}-}^{(e)}(\xi, z, i+j)] \frac{[[\langle m_{\bar{\alpha}} \rangle^2]_s]_c^{1/2}}{[x_{\bar{\alpha}}]_s}. \quad (68)$$

The energies on the right-hand side of Eq. (68) are given by

$$E_\alpha(\xi, z, l) = \int d\omega f(\omega) \frac{D}{\pi} \text{Im} \sum_\sigma \ln [\hat{L}_{\alpha\sigma}(\xi, l)^{-1} - \mathcal{L}_\sigma^{-1} + F_{00\sigma}(z, l)^{-1}] - n_\alpha \omega_\alpha(\xi, l) + \frac{1}{4} \tilde{J}_\alpha \xi^2, \quad (69)$$

$$\left[\begin{array}{c} \Phi_{\alpha\gamma\pm}^{(a)}(\xi, z, l) \\ \Phi_{\alpha\gamma\pm}^{(e)}(\xi, z, l) \end{array} \right] = \frac{1}{2} \sum_{\nu=\pm} \left[\begin{array}{c} 1 \\ -\nu \end{array} \right] \Phi_{\alpha\gamma\pm}(\xi, \nu[x_\gamma]_s, z, l), \quad (70)$$

$$\Phi_{\alpha\gamma\pm}(\xi, \nu[x_\gamma]_s, z, l) = \int d\omega f(\omega) \frac{D}{\pi} \text{Im} \sum_\sigma \ln [1 - F_{0j\sigma} F_{j0\sigma}^\pm(z, l) \tilde{t}_{\alpha\sigma}(\xi, z, l) \tilde{t}_{\gamma\sigma}(\nu[x_\gamma]_s)]. \quad (71)$$

Here

$$F_{00\sigma}(z, l) = \left[\mathcal{L}_\sigma^{-1} - \left[z + (2l - z) \frac{[(\delta y)_s]^{1/2}}{[y]_s} \right] [y]_s \mathcal{H}_\sigma \right]^{-1}, \quad (72)$$

$$F_{0j\sigma} F_{j0\sigma}^\pm(z, l) = \left[1 \pm \frac{[(\delta y)_s]^{1/2}}{[y]_s} \right] [y]_s \mathcal{H}_\sigma^2 F_{00\sigma}(z, l)^2, \quad (73)$$

$$\tilde{t}_{\alpha\sigma}(\xi, z, l) = \frac{\hat{L}_{\alpha\sigma}(\xi, l)^{-1} - \mathcal{L}_\sigma^{-1}}{1 + [\hat{L}_{\alpha\sigma}(\xi, l)^{-1} - \mathcal{L}_\sigma^{-1}] F_{00\sigma}(z, l)}, \quad (74)$$

$$\tilde{t}_{\gamma\sigma}(v[x_\gamma]_s) = \frac{\bar{L}_{\gamma\sigma}(v[x_\gamma]_s)^{-1} - \mathcal{L}_\sigma^{-1}}{1 + [\bar{L}_{\gamma\sigma}(v[x_\gamma]_s)^{-1} - \mathcal{L}_\sigma^{-1}] F_\sigma}, \quad (75)$$

$$\hat{L}_{\alpha\sigma}^{-1}(\xi, l) = \frac{\omega + i\delta - \epsilon_\alpha + \mu - w_\alpha(\xi, l) + \frac{1}{2} \tilde{J}_\alpha \xi \sigma + h\sigma}{|r_\alpha|^2}, \quad (76)$$

$$\bar{L}_{\alpha\sigma}^{-1}(\xi) = \frac{\omega + i\delta - \epsilon_\alpha + \mu - \bar{w}_\alpha(\xi) + \frac{1}{2} \tilde{J}_\alpha \xi \sigma + h\sigma}{|r_\alpha|^2}. \quad (77)$$

The charge potentials $w_\alpha(\xi, l)$ at the central site and $\bar{w}_\alpha(\xi)$ at the neighboring site are determined from the charge-neutrality condition of Eq. (40):

$$n_\alpha = \int d\omega f(\omega) \frac{-D}{\pi} \text{Im} \sum_\sigma \frac{1}{|r_\alpha|^2} [\hat{L}_{\alpha\sigma}(\xi, l)^{-1} - \mathcal{L}_\sigma^{-1} + F_{00\sigma}(z, l)^{-1}]^{-1}, \quad (78)$$

$$n_\alpha = \int d\omega f(\omega) \frac{-D}{\pi} \text{Im} \sum_\sigma \frac{1}{|r_\alpha|^2} [\bar{L}_{\alpha\sigma}(\xi)^{-1} - \mathcal{L}_\sigma^{-1} + F_\sigma^{-1}]^{-1}. \quad (79)$$

The average amplitude $[x_\alpha]_s$ is given in the present scheme as

$$[x_\alpha]_s = \sum_z p_\alpha(z) \sum_{l=0}^z \Gamma(l, z, \frac{1}{2}) x_\alpha(z, l), \quad (80)$$

$$x_\alpha(z, l)^2 = \frac{\int d\xi \xi^2 e^{-\beta E_\alpha(\xi, z, l)}}{\int d\xi e^{-\beta E_\alpha(\xi, z, l)}}. \quad (81)$$

With use of the same approximation scheme, the CPA equation is expressed as follows:

$$\sum_\alpha c_\alpha \sum_{\nu=\pm} \frac{1}{2} \left[1 + \nu \frac{[[\langle \xi_\alpha \rangle]_s]_c}{[[\langle \xi_\alpha^2 \rangle]_s]_c^{1/2}} \right] \{ \bar{L}_{\alpha\sigma}(v[[\langle \xi_\alpha^2 \rangle]_s]_c^{1/2})^{-1} - \mathcal{L}_\sigma^{-1} + F_\sigma^{-1} \}^{-1} = F_\sigma, \quad (82)$$

$$\begin{aligned} \left[\frac{[[\langle \xi_\alpha \rangle]_s]_c}{[[\langle \xi_\alpha^2 \rangle]_s]_c} \right] &= \sum_z p_\alpha(z) \sum_{n=0}^z \Gamma(n, z, p^{\alpha\alpha}) \sum_{i=0}^n \Gamma(i, n, \frac{1}{2}) \sum_{j=0}^{z-n} \Gamma(j, z-n, \frac{1}{2}) \\ &\quad \times \sum_{k_1=0}^i \Gamma(k_1, i, q_\alpha) \sum_{k_2=0}^{n-i} \Gamma(k_2, n-i, q_\alpha) \sum_{l_1=0}^j \Gamma(l_1, j, q_{\bar{\alpha}}) \\ &\quad \times \sum_{l_2=0}^{z-n-j} \Gamma(l_2, z-n-j, q_{\bar{\alpha}}) \left[\frac{\langle \xi_\alpha \rangle(z, n, i, j, k_1, k_2, l_1, l_2)}{\langle \xi_\alpha^2 \rangle(z, n, i, j, k_1, k_2, l_1, l_2)} \right], \end{aligned} \quad (83)$$

$$\langle \xi_\alpha^2 \rangle(z, n, i, j, k_1, k_2, l_1, l_2) = \frac{\int d\xi \xi^2 e^{-\beta \Psi(\xi, z, n, i, j, k_1, k_2, l_1, l_2)}}{\int d\xi e^{-\beta \Psi(\xi, z, n, i, j, k_1, k_2, l_1, l_2)}}. \quad (84)$$

Magnetic states of amorphous alloys at finite temperatures are obtained by solving Eq. (66) for $[[\langle m_\alpha \rangle]_s]_c$ and $[[\langle m_\alpha \rangle^2]_s]_c$, and Eq. (82) for the effective medium \mathcal{L}_σ self-consistently with additional equations (51), (78), and (79).

D. Discussion on the choice of parameters

In the present theory, the following parameters are needed in the numerical calculations.

(1) The average DOS for noninteracting electrons in amorphous pure metals $\{[\rho_\alpha(\epsilon)]_s\}$.

(2) The d electron numbers $\{n_\alpha\}$ and the effective exchange energy parameters $\{\tilde{J}_\alpha\}$.

(3) The average coordination numbers $\{z_\alpha^*\}$ and ASRO parameters $\{\tau_\alpha\}$.

(4) The fluctuations of the square of the transfer integrals $[(\delta\theta)^2]_s/[\theta]_s^2$ or $[(\delta y)^2]_s/[y]_s^2$, and the average square of transfer integrals $\{[y_\alpha]_s\}$.

(5) The factor $|r_\alpha|$ in the GM model.

Among these parameters, $\{[\rho_\alpha(\epsilon)]_s\}$ are immediately obtained from the first-principles calculations for amorphous pure metals. The d electron numbers $\{n_\alpha\}$ are also estimated from the results of calculations. The effective exchange energy parameters $\{\tilde{J}_\alpha\}$ are chosen so that the obtained magnetization for crystalline counterparts is reproduced. Otherwise we can take the value estimated from band calculations.

There is a relation among $\{z_\alpha^*\}$ and $\{\tau_\alpha\}$, which is obtained from a consistency for the number of neighboring A - B pairs.

$$z_A^*(1-\tau_A) = z_B^*(1-\tau_B). \quad (85)$$

The above relation means that we cannot consider the case of complete disorder ($\tau_A = \tau_B = 0$) in amorphous alloys when the size of atom A is different from that of atom B because the atomic-size difference leads to $z_A^* \neq z_B^*$. We therefore consider the case of the most random atomic configuration under the condition of Eq. (85). This condition is (see Appendix A)

$$c_A \tau_B + c_B \tau_A = 0. \quad (86)$$

Moreover, we assume a linear relation between z_α^* and $p^{\alpha\alpha}$:

$$z_\alpha^* = z_\alpha^*(0) + p^{\alpha\alpha} [z_\alpha^*(1) - z_\alpha^*(0)]. \quad (87)$$

Here the average coordination numbers $z_\alpha^*(0)$ and $z_\alpha^*(1)$ are the values for $p^{\alpha\alpha} = 0$ and $p^{\alpha\alpha} = 1$, which are estimated approximately from the dense random packing of hard-spheres (DRPHS) model. This relation means that the coordination number of atoms with larger size increases linearly with decreasing the same type of neighboring atoms. For further discussion on this relation, see Appendix B.

The fluctuations of structure via $[(\delta\theta)^2]_s/[\theta]_s^2$ are calculated as follows:

$$\begin{aligned} [\theta]_s &= \sum_z p(z) \int \left[\sum_{j \neq 0}^z y_j \right] \left[\prod_j p_s(y_j) dy_j \right] \\ &= z^* [y]_s, \end{aligned} \quad (88)$$

$$\begin{aligned} [(\delta\theta)^2]_s &= \sum_z p(z) \int \left[\sum_{j \neq 0}^z y_j - [\theta]_s \right]^2 \left[\prod_j p_s(y_j) dy_j \right] \\ &= \sum_z p(z) \left[\sum_{i,j \neq 0} [\delta y_i \delta y_j]_s + (\delta z)^2 [y]_s^2 \right]. \end{aligned} \quad (89)$$

Here $p(z)$ denotes the distribution function of z , and $z^* [= z_\alpha^*(1)]$ is the average coordination number of amorphous pure metal. In the Bethe-type approximation, $[\delta y_i \delta y_j]_s = 0$ ($i \neq j$). Thus, we have

$$\frac{[(\delta\theta)^2]_s}{[\theta]_s^2} = \left[\frac{[(\delta y)^2]_s}{z^* [y]_s^2} + \frac{[(\delta z)^2]_s}{z^{*2}} \right]. \quad (90)$$

The first term on the right-hand side of Eq. (90) can be estimated from the fluctuations of the NN interatomic distance $[(\delta R)^2]_s/[R]_s^2$:

$$\frac{[(\delta y)^2]_s}{[y]_s^2} = 4\kappa^2 \frac{[(\delta R)^2]_s}{[R]_s^2}, \quad (91)$$

which is obtained from the width of the first peak of the pair distribution function in experiment or computer simulation. The second term is neglected in the following calculations because $p_\alpha(z)$ in Eq. (61) does not describe the fluctuations $[(\delta z)^2]_s/z^{*2}$ correctly. The average square of transfer integrals $[y_\alpha]_s$ is calculated from the second moment [see Eq. (57)]:

$$z^* [y_\alpha]_s = \mu_2(\alpha). \quad (92)$$

The factor $|r_\alpha|$ defined by Eq. (42) is also obtained from the second moment $\mu_2(\alpha)$ as follows:

$$|r_\alpha|^2 = \begin{cases} [\mu_2(A)/\mu_2(B)]^{1/2} & \text{for } \alpha = A, \\ 1 & \text{for } \alpha = B. \end{cases} \quad (93)$$

Finally, we briefly mention the calculation scheme in obtaining the self-consistent solutions. After fixing the parameters mentioned above, we first assume $[[\langle m_\alpha \rangle]_s]_c$, $[[\langle m_\alpha \rangle^2]_s]_c^{1/2}$, $[[\langle \xi_\alpha^2 \rangle]_s]_c^{1/2}$, and $\bar{w}_\alpha(\pm[[\langle \xi_\alpha^2 \rangle]_s]_c^{1/2})$, and solve the CPA equation [Eq. (82)]. Next we calculate \mathcal{H}_σ , $F_{00\sigma}$, and $F_{0j\sigma} F_{j0\sigma}^\pm$ from Eqs. (51), (72), and (73), and solve Eqs. (78) and (79) for the charge potentials $w_\alpha(\xi, l)$ and $\bar{w}_\alpha(\xi)$. Therefore, we can obtain the new values $[[\langle m_\alpha \rangle]_s]_c$ and $[[\langle m_\alpha \rangle^2]_s]_c^{1/2}$ solving Eq. (66) by means of the iteration method and then calculate the new values of $[[\langle \xi_\alpha^2 \rangle]_s]_c^{1/2}$ and $\bar{w}_\alpha(\pm[[\langle \xi_\alpha^2 \rangle]_s]_c^{1/2})$ from Eqs. (83) and (79). This procedure should be repeated until self-consistency is achieved.

III. NUMERICAL RESULTS

Characteristic features of the present theory are the description of itinerant-electron SG and the inclusion of atomic-size effects via the difference in the average coordination numbers of constituent atoms. To test the validity of these new aspects, we have performed the numerical calculations for the amorphous Fe-Zr alloys, which consist of $3d$ and $4d$ TM with distinct difference in atomic size and show the SG-ferromagnet transition.

The input DOS for amorphous Fe and Zr metals are

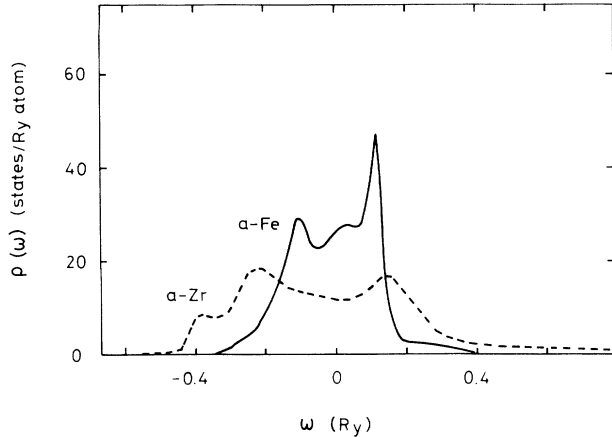


FIG. 1. The input densities of states (DOS) for the amorphous Fe (Ref. 41) (solid curve) and the amorphous Zr (dashed curve) calculated with use of the tight-binding LMTO recursion method.

shown in Fig. 1. The former is taken from the results obtained by Fujiwara,⁴¹ and the latter was calculated by Tanaka. In both cases, the amorphous structures were generated by using the relaxed DRPHS model with 1500 atoms, and the electronic structures were calculated by means of a tight-binding linear muffin-tin orbital (LMTO) recursion method.

In the 3d-4d TM alloys, a change in the *d* electron number is expected with varying concentration because of the considerable difference in the atomic level between the 3d and 4d atoms. In fact, we have calculated the electronic structures for nonmagnetic amorphous Fe₉₀Zr₁₀ and Fe₆₅Zr₃₅ alloys with use of the tight-binding LMTO recursion method, and found a change in the *d* electron number: $n_{\text{Fe}}(c_{\text{Fe}}=0.65) - n_{\text{Fe}}(c_{\text{Fe}}=0.90) = 0.43$, though the charge neutrality still holds true in the atomic spheres. We therefore adopt the concentration dependence of the *d* electron number for Fe as $n_{\text{Fe}} = 7.0 + (1.0 - c_{\text{Fe}})0.5$, while the *d* electron number for Zr is assumed to be constant as $n_{\text{Zr}} = 3.0$ since the magnetic properties are not so sensitive to a small change in the Zr part. The set of *d* electron numbers leads to a reasonable peak position of Fe local DOS at low Fe concentrations as will be shown later.

The effective exchange energy parameters are chosen to be $\tilde{J}_{\text{Fe}} = 0.064$ Ry and $\tilde{J}_{\text{Zr}} = 0.046$ Ry. The former is chosen so that the critical concentration for the disappearance of ferromagnetism is consistent with the experimental data.^{5,13,14} This value gives the ground-state magnetization $2.3\mu_B$ for bcc Fe. The latter is taken from Janak's paper.⁴²

Moreover, we adopt $[(\delta R)^2]_s^{1/2}/[R]_s = 0.06$ for both amorphous Fe and Zr. This value was estimated from the experimental data⁴³ and the theoretical calculation⁴⁴ for the pair distribution functions of amorphous Fe.

The average coordination numbers $\{z_{\alpha}^*\}$ and ASRO parameters $\{\tau_{\alpha}\}$ shown in Fig. 2 are determined from the following parameters via Eqs. (85)–(87): $z_{\text{Fe}}^*(0) = 7.0$, $z_{\text{Zr}}^*(0) = 16.0$, and $z_{\text{Fe}}^*(1) = z_{\text{Zr}}^*(1) = 11.5$. They are estimated from the view point of the DRPHS model.

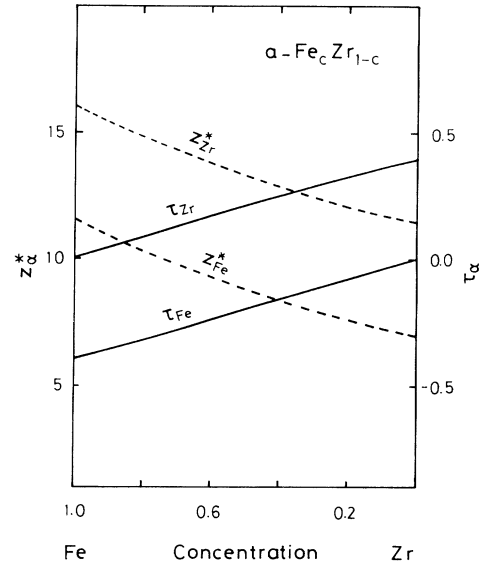


FIG. 2. The concentration dependences of the ARSO parameters $\{\tau_{\alpha}\}$ (solid lines) and the average coordination numbers $\{z_{\alpha}^*\}$ (dashed lines) obtained from the condition of the most random atomic configuration and a linear equation for $\{z_{\alpha}^*\}$ [see Eqs. (85)–(87)].

We first illustrate, in Figs. 3(a)–3(e), the average local DOS calculated at 75 K (see Appendix C for the expression). The Fe local DOS form the Lorentz-like narrow band in the broad 4d band around 35 at. % Fe. With increasing Fe concentration, the bandwidth of Fe local DOS gradually increases, and the local DOS polarize with the appearance of ferromagnetism. Moreover, it is seen that the down-spin bandwidth for Fe local DOS becomes larger than the up-spin one because of more mixing of the former with the Zr bands. In the Fe-rich region, magnetization rapidly decreases beyond 85 at. % Fe, and the SG state appears after the disappearance of ferromagnetism. The local DOS in the SG state is presented in Fig. 3(e).

Recently, Turek *et al.*³⁰ have performed the ground-state electronic structure calculations for amorphous Fe-Zr alloys with use of the LMTO-supercell approach, in which they constructed the amorphous structure from 64 atoms in a box with the periodic boundary condition by making use of the molecular dynamics method, and calculated the spin-polarized DOS for the amorphous Fe-Zr compounds with use of the same periodic boundary condition. Their results are also drawn in Figs. 3(a)–3(e). We find that our results are in good agreement with their results for 35, 50, 65, and 75 at. % Fe, where there is not as much competition between ferromagnetic and antiferromagnetic interactions. This supports that the present theory with the most random atomic configuration describes semiquantitatively or even quantitatively the average local DOS in amorphous TM alloys.

The exception is found beyond 90 at. % Fe, where our result shows the SG state, while Turek's result still shows the ferromagnetism. The same discrepancy was found even in amorphous pure Fe, in which their results show a F-P transition at very high density 10.2 g/cm³, and do not show the SG at any volume.⁴⁵ This seems to be relat-

ed to the different number of configurations and the different self-consistency between the two schemes. The number of configurations in the NN cluster is about $2 \times 2^2 \times 2^2 \times 2^2 (\sim 10^{11})$ in our scheme, while it is less than

10^2 (64 atoms in a unit cell) in their scheme.³⁰ The latter is probably insufficient to describe a reasonable phase transition such as the transition from ferromagnetism to SG, though they chose the most probable configuration.

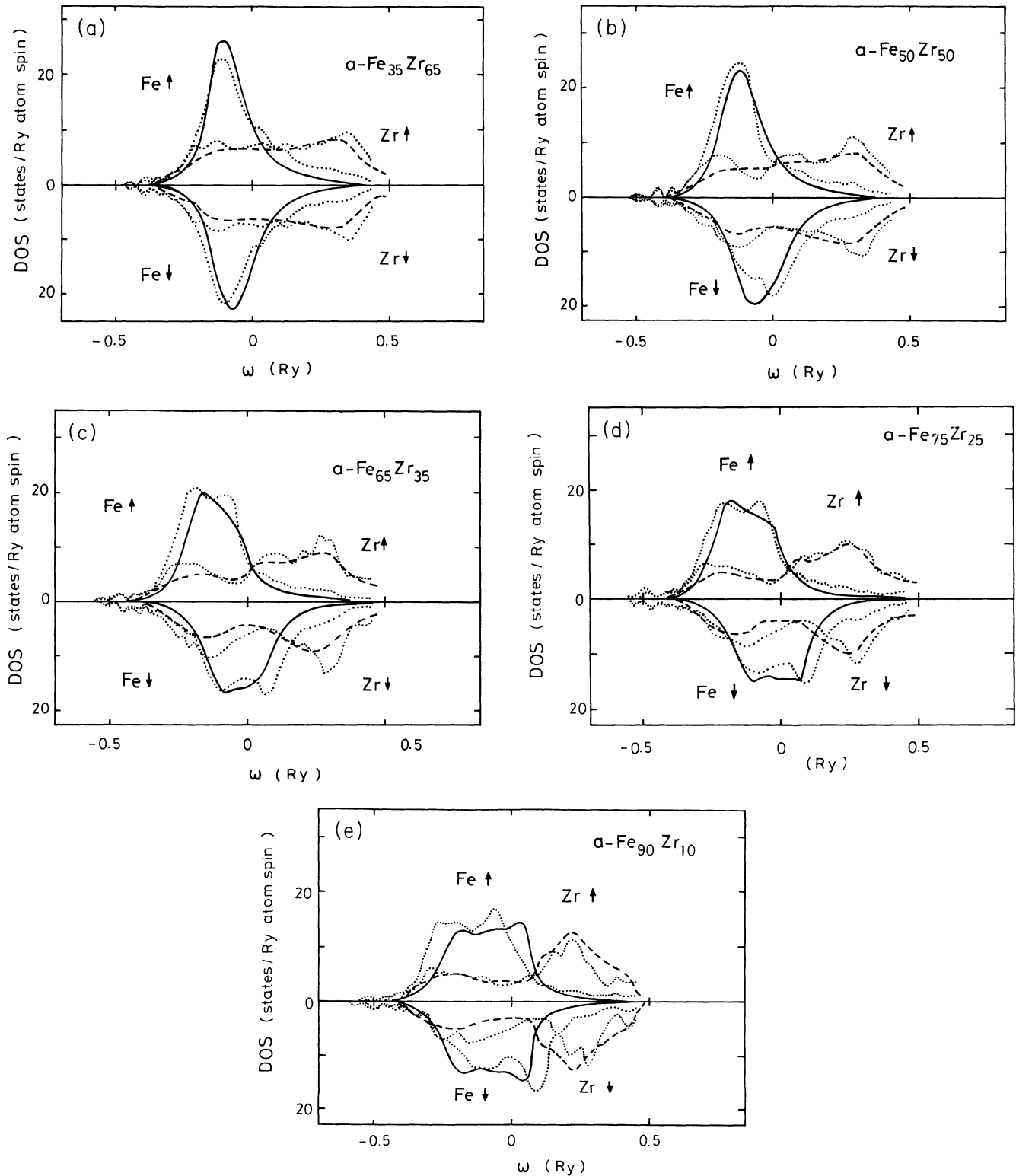


FIG. 3. Calculated average local DOS for Fe (solid curves) and Zr (dashed curves) atoms at 75 K. Dotted curves show the local DOS obtained by Turek *et al.* (Ref. 30) at the same concentrations except (a) (33 at. % Fe) and (c) (67 at. % Fe).

Another point which we would like to discuss is that the unit cell of magnetic structure is generally larger than that of crystal structure, especially in the system with competition between ferromagnetic and antiferromagnetic interactions. In that case, the same periodicity as that in the crystal structure may lead to an overestimate of magnetization. In fact, the ground-state magnetization of fcc Fe-Ni alloys calculated with use of the same approach⁴⁶ remains finite over all concentrations, while the experimental data indicate the appearance of a SG around 70 at. % Fe.⁴⁷ In our theory, calculated magnetization disappears around 70 at. % Fe, and the SG state is realized being consistent with the experimental data because of the self-consistent treatment of the LM's without use of the periodic boundary condition.⁴⁸

The temperature dependence of an average local DOS for the amorphous Fe₇₅Zr₂₅ alloys is presented in Fig. 4. With increasing temperature, the splitting between the up-spin and down-spin bands for Fe gradually decreases and vanishes above T_C . The disappearance of average exchange splitting causes more (less) mixing of the up-spin (down-spin) band for Fe with the Zr band, and the thermal spin fluctuations tend to broaden both up- and down-spin bands, so that the up-spin bandwidth becomes broader as temperature increases, while the down-spin bandwidth is almost independent of temperature.

In Fig. 5, we present our numerical result for the magnetic phase diagram in the temperature-concentration plane. The present theory with the condition of the most random atomic configuration describes well the three different phases P, F, and SG. In particular, it suggests the existence of RSG behavior in a narrow range of concentration near the SG-F phase boundary in the Fe-rich region, in agreement with the experimental data by Fukamichi *et al.*⁴ (see the inset of Fig. 5). In our results, the maximum of calculated T_C is 420 K at 70 at. % Fe, which should be compared with the experimental value 275 K. Calculated T_g increase linearly from 150 K at the triple point (85 at. % Fe) to 240 K at amorphous Fe with

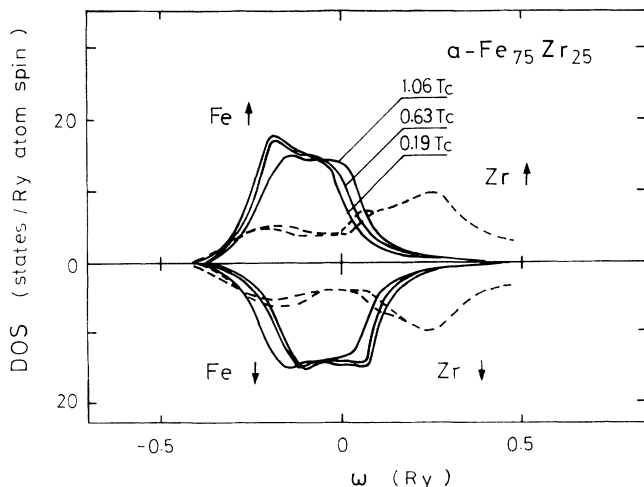


FIG. 4. Calculated average local DOS for amorphous Fe₇₅Zr₂₅ alloys at various temperatures. The average local DOS for the Zr part at 0.63 T_C lie between the asymmetric DOS at 0.19 T_C and the symmetric one at 1.06 T_C .

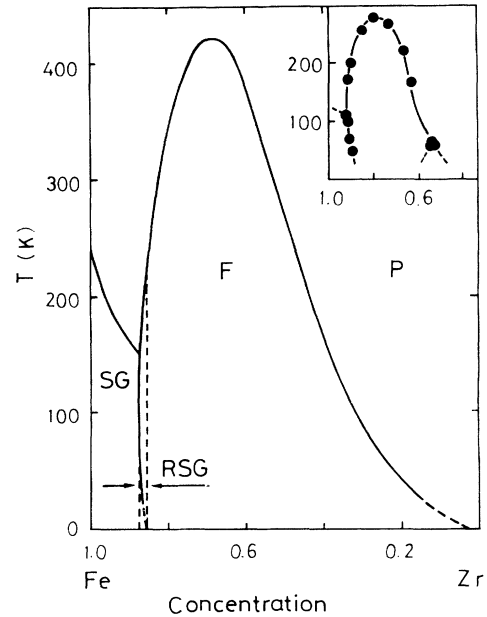


FIG. 5. Calculated magnetic phase diagram of amorphous Fe-Zr alloys, showing paramagnetism (P), ferromagnetism (F), spin-glass (SG), and reentrant spin-glass (RSG). The inset shows the experimental results by Fukamichi *et al.* (Ref. 4). Curie-temperatures (T_C) and spin-glass transition temperatures (T_g) below 50 K are expected by dashed lines.

increasing Fe concentration. These transition temperatures are overestimated by a factor of 1.5–2.0 as compared with the experimental ones, which is mainly attributed to the molecular-field approximation used in the present theory.⁴⁰ The magnetic properties below 50 K have not been obtained yet because of the numerical difficulties at low temperatures. The SG state which may appear below 50 at. % Fe according to the experimental data⁴ has not been found. We therefore concentrate the following discussions on the formation of SG and RSG behaviors in the Fe-rich region.

The SG state in amorphous Fe has been clarified by Kakehashi^{26,27} from the viewpoint of structural disorder. He found that the SG behaviors change with the d electron number N . In the range of $6.8 \lesssim N \lesssim 7.2$, the formation of SG is attributed to the competition between ferromagnetic and antiferromagnetic NN interactions, which is caused by the nonlinear magnetic couplings between the NN LM's and the LEE's on the amplitudes of LM's. However, the SG's in the range $7.2 \lesssim N \lesssim 7.35$ were found to accompany the ferromagnetic clusters because of the disappearance of antiferromagnetic NN interactions. The SG's, therefore, are caused by the competition between the NN ferromagnetic interactions and long-range antiferromagnetic interactions.

The formation of a SG in the amorphous Fe-Zr alloys seems to be between the former and the latter cases mentioned above. In fact, the nonlinear magnetic couplings between the NN Fe LM's are found in the Fe-Fe exchange pair energies $-\Phi_{\text{FeFe}\pm}^{(e)}(\xi, l)$ when the number of contracted atoms (l) are larger than 5 (see Fig. 6); the central Fe LM with small amplitude antiferromagnetic-

ly couples to the neighboring Fe LM's, but the central Fe LM with large amplitude ferromagnetically couples to the neighboring Fe LM's. Thus, the nonlinear magnetic couplings can bring about a coexistence of ferromagnetic and antiferromagnetic interactions between the central and the neighboring Fe LM's because there is a broad distribution of the amplitudes of Fe LM's ($\langle \xi_{\text{Fe}}^2 \rangle^{1/2}$) whose width is about $2.4\mu_B$ as seen from Fig. 7. On the other hand, we found rather strong ferromagnetic correlation between the central $\langle m_{0\text{Fe}} \rangle$ and neighboring $\langle m_{1\text{Fe}} \rangle$ Fe LM's (i.e., $[[\langle m_{0\text{Fe}} \rangle \langle m_{1\text{Fe}} \rangle]_s]_c (c_{\text{Fe}} = 0.9) = 0.15$ at 75 K). This means that the NN ferromagnetic interactions are rather strong as compared with the NN antiferromagnetic ones. Therefore, the existence of long-range antiferromagnetic interactions seems to be plausible, and it is found, indeed, by examining the response of the central Fe LM when we polarize the effective medium. This is in favor of the formation of cluster SG in the amorphous Fe-Zr alloys in the Fe-rich region.

The RSG behavior appears near the SG-F boundary in the Fe-rich region (see Fig. 5), which is mainly attributed to the thermal spin fluctuations of amplitude of Fe LM's because of the following reason. The magnetic couplings $[-\Phi_{\text{FeFe}\pm}^{(e)}(\xi, l)]$ between the central and the neighboring Fe LM's are governed by an average amplitude of neighboring Fe LM's ($[x_{\text{Fe}}]_s$) and the effective medium \mathcal{L}_σ which is again determined by the average amplitudes $[[\langle \xi_{\text{Fe}}^2 \rangle]_s]_c^{1/2}$ via CPA Eq. (82) in the SG states. When the temperature is elevated, the thermal spin fluctuations increase the amplitude $[x_{\text{Fe}}]_s$. This makes the exchange pair energies $[-\Phi_{\text{FeFe}\pm}^{(e)}(\xi, l)]$ more ferromagnetic and unbalances the competition between short-range ferromagnetic and long-range antiferromagnetic interactions, so that a net magnetization appears at the RSG temperatures. The mechanism, therefore, seems to be the same as that found in the theoretical investigations for amorphous TM's.^{26,27}

When the Fe concentration decreases, smaller Fe atoms are replaced by larger Zr atoms on the NN shell of the Fe atom. This leads to a decrease of the average

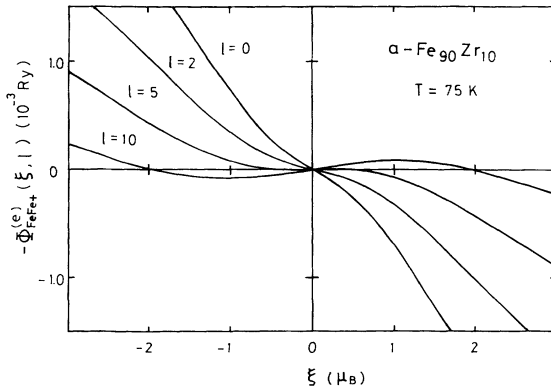


FIG. 6. Exchange Fe-Fe pair energies $[-\Phi_{\text{FeFe}\pm}^{(e)}(\xi, l)]$ for various environments l (the number of contracted atoms on the NN shell). They show a magnetic energy gain for the central Fe LM when the neighboring Fe LM's with amplitudes $[x_{\text{Fe}}]_s$ point up [see Eq. (20)].

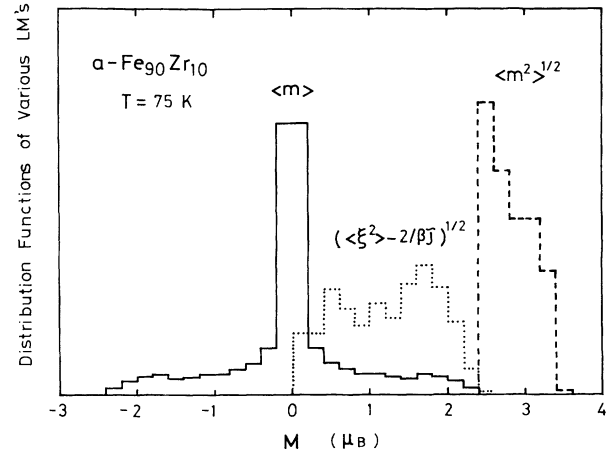


FIG. 7. The distribution functions of various LM's: $\langle m \rangle$ (solid curve), $\langle m^2 \rangle^{1/2}$ (dashed curve), and $(\langle \xi^2 \rangle - 2/\beta J)^{1/2}$ (dotted curve) for amorphous $\text{Fe}_{90}\text{Zr}_{10}$ alloys at 75 K.

coordination number z_{Fe}^* according to the DRPHS model (see Fig. 2), and therefore causes additional band narrowing in the Fe local DOS since the second moment is proportional to z_{Fe}^* . We present, in Fig. 8, as an example, two kinds of local DOS for the nonmagnetic amorphous $\text{Fe}_{65}\text{Zr}_{35}$ alloys to show the effects on magnetism: the local DOS with atomic-size effects under the most random atomic configuration ($z_{\text{Fe}}^* = 9.5$, $z_{\text{Zr}}^* = 14.0$, $\tau_{\text{Fe}} = -0.26$, $\tau_{\text{Zr}} = 0.14$) and the local DOS with the same atomic size ($z_{\text{Fe}}^* = z_{\text{Zr}}^* = 12.0$, $\tau_{\text{Fe}} = \tau_{\text{Zr}} = 0.0$). The former shrinks the bandwidth at the Fe site and develops the peak near the Fermi level in the Fe local DOS as compared with the latter. These changes in the local DOS are favorable for the enhancement of ferromagnetism. In fact, we obtained the magnetization $0.75\mu_B$ at 75 K, which is reasonable for the experimental data [$0.95\mu_B$ at 4 K (Ref. 15)]. However, we did not find the appearance of ferromagne-

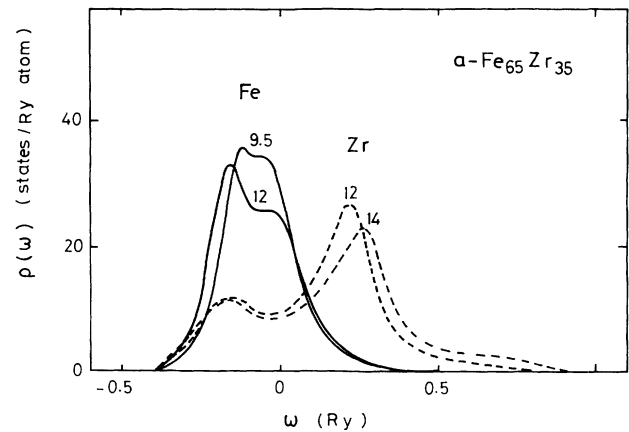


FIG. 8. Local DOS for Fe (solid curves) and Zr (dashed curves) atoms in the nonmagnetic state at 65 at. % Fe, which are calculated by the ground-state theory (Ref. 23). The average coordination numbers $\{z_a^*\}$ are shown on the curves which correspond to the case of the most random atomic configuration ($z_{\text{Fe}}^* = 9.5$, $z_{\text{Zr}}^* = 14.0$, $\tau_{\text{Fe}} = -0.26$, $\tau_{\text{Zr}} = 0.14$) and the case of the same atomic size ($z_{\text{Fe}}^* = z_{\text{Zr}}^* = 12.0$, $\tau_{\text{Fe}} = \tau_{\text{Zr}} = 0.0$), respectively.

tism in the case of the same atomic size. Thus, the large difference in atomic size between Fe and Zr atoms plays an important role in the formation of ferromagnetism in the amorphous Fe-Zr alloys.

IV. SUMMARY

We have developed a finite-temperature theory for amorphous magnetic alloys on the basis of the functional integral method and the distribution-function method. The theory drastically reduces the numerical calculations for amorphous structure and electronic structure by means of the GM model outside a cluster. It allows us to investigate theoretically the amorphous magnetic alloys with a large difference in atomic size at arbitrary concentration using a small number of parameters for amorphous pure metals and local atomic configurations. It reduces to the previous theory^{38,40,49} in the case of substitutional alloys, which succeeded in explaining the Slater-Pauling curves, the Curie-temperature Slater-Pauling curves, and the effective Bohr magneton numbers for 3d TM alloys. It also recovers the recent theory²⁵⁻²⁷ in the limit of amorphous pure metals, which has described systematic change in magnetism of amorphous 3d TM's. Thus, the present theory covers a wide range of magnetism.

We have applied this theory to the amorphous Fe-Zr alloys to demonstrate its reliability. Calculated local DOS at low temperatures reproduced well those obtained from the first-principles LMTO-supercell approach.³⁰ The new parameters z_α^* explained the formation of ferromagnetism due to the atomic-size effects in amorphous Fe-Zr alloys. The self-consistent equations for LM's ($[\langle m_\alpha \rangle]_s]_c$ and $[\langle m_\alpha^2 \rangle]_s]_c^{1/2}$) reproduced the itinerant-electron SG as well as the RSG in the Fe-rich region. In particular, we found that the RSG is caused by the thermal spin fluctuations of amplitudes which are never seen in the insulators. It was also shown that the most random atomic configuration reproduces the magnetic phase diagram in amorphous Fe-Zr alloys. The numerical results mentioned above encourage us to perform systematic investigations for 3d-4d and 3d-5d amorphous alloys on the basis of the present theory.

Finally, we remark that although we have succeeded in explaining the overall feature of magnetic phase diagram in amorphous Fe-Zr alloys, there are still some problems which should be examined in the future. For example, we have not taken into account the magnetic couplings between the central and next-NN LM's in the present theory, which may be expected to hold the key to the formation of SG in amorphous Fe-Zr alloys below 50 at. % Fe. We also have neglected the transverse components of spin fluctuations. It not only underestimates the magnetic entropy, but also excludes the possibility of transverse spin freezing as found in the classical Heisenberg model.⁵⁰⁻⁵² Moreover, we have neglected the amplitude fluctuations $[\langle (\delta x_\alpha)^2 \rangle]_s]_c$ on the neighboring sites in our self-consistent equations. This effect seems to be important near the critical concentration of ferromagnetic instability since the amplitudes of LM's are expected to change drastically there. These problems should be solved in fu-

ture investigations to reach a more solid conclusion in this field.

ACKNOWLEDGMENTS

The authors would like to thank Professor K. Fukamiuchi, Professor N. Kataoka, and Dr. A. Fujita for valuable discussions. This work was partly supported by a Grant-in-Aid Scientific Research from the Ministry of Education, Science, and Culture in Japan.

APPENDIX A:

THE MOST RANDOM ATOMIC CONFIGURATION

When the average coordination numbers are not equal to each other (i.e., $z_A^* \neq z_B^*$), the condition of complete disorder ($\tau_A = \tau_B = 0$) cannot be realized according to Eq. (85). We therefore consider here the most random atomic configuration which leads to the least mean square of deviation ($p^{\alpha\gamma} - c_\gamma$) from the complete disorder ($p^{\alpha\gamma} = c_\gamma$).

We first define a mean square of derivations taken over all the NN pairs:

$$L \equiv \frac{1}{2} N \sum_\alpha c_\alpha \sum_\gamma z_\alpha^* p^{\alpha\gamma} (p^{\alpha\gamma} - c_\gamma)^2. \quad (\text{A1})$$

Here $z^* p^{\alpha\gamma}$ denotes the number of α - γ pairs around an α atom, and N is the total number of sites. To minimize Eq. (A1) under the condition of Eq. (85), we introduce a Lagrangian multiplier λ :

$$\Phi \equiv L + \lambda [(1 - \tau_\alpha) z_\alpha^* - (1 - \tau_{\bar{\alpha}}) z_{\bar{\alpha}}^*]. \quad (\text{A2})$$

Minimizing the new function Φ with respect to $\{\tau_\alpha\}$, we obtain the following equations:

$$\frac{\partial \Phi}{\partial \tau_\alpha} = 2c_\alpha z_\alpha^* c_{\bar{\alpha}}^2 \tau_\alpha - \lambda z_\alpha^* = 0, \quad (\text{A3})$$

$$\frac{\partial \Phi}{\partial \tau_{\bar{\alpha}}} = 2c_{\bar{\alpha}} z_{\bar{\alpha}}^* c_\alpha^2 \tau_{\bar{\alpha}} + \lambda z_{\bar{\alpha}}^* = 0. \quad (\text{A4})$$

Eliminating λ in Eqs. (A3) and (A4), we finally obtain the condition of the most random atomic configuration:

$$c_\alpha \tau_{\bar{\alpha}} + c_{\bar{\alpha}} \tau_\alpha = 0. \quad (\text{A5})$$

This condition is identical with that of complete chemical disorder obtained by Cargill and Spaepen, maximizing the mixing entropy.⁵³

APPENDIX B: A SIMPLE RELATION BETWEEN THE COORDINATION NUMBER AND THE ASRO PARAMETER

It is expected from a viewpoint of the DRPHS model that the coordination number z of the α atom is strongly correlated with the number of α atoms n on the NN shell. We here argue a simple relation between the average coordination number z_α^* and the ASRO parameter τ_α in the strong-correlation limit.

Let us introduce a probability $p_\alpha(n)$ of finding n atoms of type α on the NN shell and a probability $p_\alpha(n|z)$ of

finding a z coordination number under a given n . The average coordination number z_α^* is then expressed as

$$z_\alpha^* = \sum_n \sum_z p_\alpha(n) p_\alpha(n|z) z. \quad (\text{B1})$$

We now consider the strong-correlation limit in which the coordination number $z_\alpha(n)$ is determined by the n . Then the probability $p_\alpha(n|z)$ is given by

$$p_\alpha(n|z) = \delta_{z, z_\alpha(n)}, \quad (\text{B2})$$

and Eq. (B1) reduces to

$$z_\alpha^* = \sum_n p_\alpha(n) z_\alpha(n). \quad (\text{B3})$$

Since $z_\alpha(n)$ is expected to increase monotonically with n $R_\alpha < R_{\bar{\alpha}}$ and to decrease monotonically when $R_\alpha > R_{\bar{\alpha}}$, we assume a linear dependence of n for $z_\alpha(n)$:

$$z_\alpha(n) = z_\alpha(0) + n \frac{\Delta z_\alpha^*}{z_\alpha^*}, \quad (\text{B4})$$

where Δz_α^* is an unknown constant. Substituting Eq. (B4) into (B3), we obtain

$$z_\alpha^*(p^{\alpha\alpha}) = z_\alpha(0) + p^{\alpha\alpha} \Delta z_\alpha^*. \quad (\text{B5})$$

Here we have adopted the following relation for the average number of atoms α on the NN shell:

$$\sum_n p_\alpha(n) n = z_\alpha^* p^{\alpha\alpha}. \quad (\text{B6})$$

$z_\alpha(0)$ and Δz_α^* in Eq. (B5) are determined from both $z_\alpha^*(p^{\alpha\alpha}=0)$ and $z_\alpha^*(p^{\alpha\alpha}=1)$ limits. Thus, we have

$$z_\alpha^* = z_\alpha^*(0) + p^{\alpha\alpha} \Delta z_\alpha^*, \quad (\text{B7})$$

$$\Delta z_\alpha^* = z_\alpha^*(1) - z_\alpha^*(0). \quad (\text{B8})$$

Here the average coordination number $z_\alpha^*(1)$ for an amorphous pure metal is expected to be close to 12, and the average coordination number $z_\alpha^*(0)$ for an impurity atom α in the amorphous pure metal $\bar{\alpha}$ can be estimated semiquantitatively from the DRPHS model.

APPENDIX C: LOCAL DOS

The average local DOS for σ -spin electrons on site 0 is given in the static approximation^{31,32} as follows:

$$\begin{aligned} \langle \rho_{0\sigma}(\omega) \rangle &= \left\langle \frac{-D}{\pi} \text{Im}[(L'^{-1} - t')^{-1}]_{00\sigma} \right\rangle \\ &= \left\langle \frac{D}{\pi} \frac{\partial}{\partial \epsilon_{0\sigma}} \text{Im} \text{tr}[\ln(L'^{-1} - t')] \right\rangle. \end{aligned} \quad (\text{C1})$$

Here D and $\epsilon_{0\sigma}$ denote the number of degeneracy and the atomic level on site 0, as have been explained in Sec. II. The locator matrix L' and the transfer matrix t' have been defined in Eqs. (3) and (4). The integrated electron number on the right-hand side of Eq. (C1) has appeared in the one-electron free energy in Eq. (2).

Adopting the same approximation scheme as in Sec. II, we have

$$\text{Im} \text{tr}[\ln(L' - t')^{-1}] = \text{Im} \left[\bar{X} + \sum_{(ij)} \bar{\Phi}_{ij} + \dots \right], \quad (\text{C2})$$

$$\begin{aligned} \bar{X} &= \text{tr}[\ln(\mathcal{L}_\sigma^{-1} - \hat{t})] + \sum_{i\sigma} \ln F_{ii\sigma} \\ &\quad + \sum_{i\sigma} \ln(\hat{L}_{i\sigma}^{-1} - \mathcal{L}_{i\sigma}^{-1} + F_{ii\sigma}^{-1}), \end{aligned} \quad (\text{C3})$$

$$\bar{\Phi}_{ij} = \sum_\sigma \ln[1 - \tilde{t}_{i\sigma}(\xi_i) \tilde{t}_{j\sigma}(\xi_j) F_{ij\sigma} F_{ij\sigma}]. \quad (\text{C4})$$

Here the single-site matrix $\tilde{t}_{i\sigma}(\xi_i)$ and the coherent Green's functions $\{F_{ii\sigma}, F_{ij\sigma}\}$ have been defined in Eqs. (43), (45), and (46).

The single-site term \bar{X} is stationary for a change of the effective medium (i.e., $\partial \bar{X} / \partial \mathcal{L}_{i\sigma}^{-1} = 0$) because of the CPA, Eq. (44). Therefore, we can neglect the change via $\mathcal{L}_{i\sigma}^{-1}$ in the single-site approximation. It is also obvious that one can neglect again the change via $\mathcal{L}_{i\sigma}^{-1}$ when one takes into account all the terms in the series of expansion because the result does not depend on $\mathcal{L}_{i\sigma}$. Therefore, we may neglect it even when we make the pair approximation in Eq. (C2) and neglect higher-order terms. The local DOS is then given by

$$\langle \rho_{\alpha\sigma}(\omega, \xi) \rangle = \langle \bar{\rho}_{\alpha\sigma}(\omega, \xi) \rangle + \left\langle \sum_{j \neq 0} \rho_{\alpha j \sigma}^{(2)}(\omega, \xi) \right\rangle, \quad (\text{C5})$$

$$\bar{\rho}_{\alpha\sigma}(\omega, \xi) = \frac{-D}{\pi} \text{Im} \frac{1}{|r_\alpha|^2} (\hat{L}_{\alpha\sigma}^{-1} - \mathcal{L}_{\alpha\sigma}^{-1} + F_{00\sigma}^{-1})^{-1}, \quad (\text{C6})$$

$$\begin{aligned} \rho_{\alpha j \sigma}^{(2)}(\omega, \xi) &= \frac{D}{\pi} \text{Im} \frac{1}{|r_\alpha|^2} \frac{F_{0j\sigma} F_{j0\sigma} \tilde{t}_{\alpha\sigma}(\xi) \tilde{t}_{j\sigma}(\xi_j)}{[1 - F_{0j\sigma} F_{j0\sigma} \tilde{t}_{\alpha\sigma}(\xi) \tilde{t}_{j\sigma}(\xi_j)]} \\ &\quad \times \frac{1}{(\hat{L}_{\alpha\sigma}^{-1} - \mathcal{L}_{\alpha\sigma}^{-1})[(\hat{L}_{\alpha\sigma}^{-1} - \mathcal{L}_{\alpha\sigma}^{-1}) F_{00\sigma} + 1]}. \end{aligned} \quad (\text{C7})$$

Here the site index 0 has been replaced by the type of atom α on the same site for brevity.

We next adopt the distribution-function method when we take the configurational and structural averages in Eq. (C5). Making again use of the decoupling approximation, we obtain the final form of the average local DOS as follows:

$$\begin{aligned} [[\langle \rho_{\alpha\sigma}(\omega, \xi) \rangle]_c]_c &= \sum_z p_\alpha(z) \sum_{n=0}^z \Gamma(n, z, p^{\alpha\alpha}) \sum_{i=0}^n \Gamma(i, n, \frac{1}{2}) \sum_{j=0}^{z-n} \Gamma(j, z-n, \frac{1}{2}) \\ &\quad \times \sum_{k_1=0}^i \Gamma(k_1, i, q_\alpha) \sum_{k_2=0}^{n-i} \Gamma(k_2, n-i, q_\alpha) \sum_{l_1=0}^j \Gamma(l_1, j, q_{\bar{\alpha}}) \\ &\quad \times \sum_{l_2=0}^{z-n-j} \Gamma(l_2, z-n-j, q_{\bar{\alpha}}) \langle \rho_{\alpha\sigma}(\omega, \xi, z, n, i, j, k_1, k_2, l_1, l_2) \rangle. \end{aligned} \quad (\text{C8})$$

Here

$$\begin{aligned} \rho_{\alpha\sigma}(\omega, \xi, z, n, i, j, k_1, k_2, l_1, l_2) = & \bar{\rho}_{\alpha\sigma}(\omega, \xi, z, i + j) + i\rho_{\alpha\alpha\sigma}^{(a)}(\omega, \xi, +, z, i + j) \\ & + (n - i)\rho_{\alpha\alpha\sigma}^{(a)}(\omega, \xi, -, z, i + j) + j\rho_{\alpha\bar{\alpha}\sigma}^{(a)}(\omega, \xi, +, z, i + j) + (z - n - j)\rho_{\alpha\bar{\alpha}\sigma}^{(a)}(\omega, \xi, -, z, i + j) \\ & - [(2k_1 - i)\rho_{\alpha\alpha\sigma}^{(e)}(\omega, \xi, +, z, i + j) + (2k_2 - n + i)\rho_{\alpha\alpha\sigma}^{(e)}(\omega, \xi, -, z, i + j)] \frac{[[\langle m_\alpha \rangle^2]_s]_c^{1/2}}{[x_\alpha]_s} \\ & - [(2l_1 - j)\rho_{\alpha\bar{\alpha}\sigma}^{(e)}(\omega, \xi, +, z, i + j) \\ & + (2l_2 - z + n + j)\rho_{\alpha\bar{\alpha}\sigma}^{(e)}(\omega, \xi, -, z, i + j)] \frac{[[\langle m_{\bar{\alpha}} \rangle^2]_s]_c^{1/2}}{[x_{\bar{\alpha}}]_s}, \end{aligned} \quad (C9)$$

$$\bar{\rho}_{\alpha\sigma}(\omega, \xi, z, l) = \frac{-D}{\pi} \text{Im} \frac{1}{|r_\alpha|^2} [\hat{L}_{\alpha\sigma}(\omega, \xi, l)^{-1} - \mathcal{L}_\sigma^{-1} + F_{00\sigma}(\omega, \xi, l)]^{-1}, \quad (C10)$$

$$\begin{bmatrix} \rho_{\alpha\gamma\sigma}^{(a)}(\omega, \xi, \pm, z, l) \\ \rho_{\alpha\gamma\sigma}^{(e)}(\omega, \xi, \pm, z, l) \end{bmatrix} = \frac{1}{2} \sum_{\nu=\pm} \begin{bmatrix} 1 \\ -\nu \end{bmatrix} \rho_{\alpha\gamma\sigma}^{(2)}(\omega, \xi, \pm, \nu[x_\gamma]_s, z, l), \quad (C11)$$

$$\begin{aligned} \rho_{\alpha\gamma\sigma}^{(2)}(\omega, \xi, \pm, \nu[x_\gamma]_s, z, l) = & \frac{D}{\pi} \text{Im} \frac{1}{|r_\alpha|^2} \frac{F_{0j\sigma} F_{j0\sigma}^\pm(z, l) \tilde{t}_{\alpha\sigma}(\xi, l) \tilde{t}_{\gamma\sigma}(\nu[x_\gamma]_s)}{[1 - F_{0j\sigma} F_{j0\sigma}^\pm(z, l) \tilde{t}_{\alpha\sigma}(\xi, l) \tilde{t}_{\gamma\sigma}(\nu[x_\gamma]_s)]} \\ & \times \frac{1}{\{\hat{L}_{\alpha\sigma}(\omega, \xi, l)^{-1} - \mathcal{L}_\sigma^{-1}\} F_{00\sigma}(z, l) + 1} \frac{1}{[\hat{L}_{\alpha\sigma}(\omega, \xi, l)^{-1} - \mathcal{L}_\sigma^{-1}]}. \end{aligned} \quad (C12)$$

The coherent Green's functions, the single-site t matrices, and the locator in Eqs. (C10)–(C12) are given by Eqs. (72)–(76).

-
- ¹F. E. Luborsky, in *Ferromagnetic Materials*, edited by K. H. J. Buschow and E. P. Wohlfarth (North-Holland, Amsterdam, 1980), Vol. 1, p. 451.
- ²K. Moorjani and J. M. D. Coey, *Magnetic Glasses* (Elsevier, Amsterdam, 1984).
- ³H. Hiroyoshi and K. Fukamichi, *Phys. Lett.* **85A**, 242 (1981); *J. Appl. Phys.* **53**, 2226 (1982).
- ⁴K. Fukamichi, T. Goto, H. Komatsu, and H. Wakabayashi, in *Proceedings of the Fourth International Conference on The Physics of Magnetic Materials*, Poland, 1988, edited by W. Gorkowski, H. K. Lachowics, and H. Szymczak (World Scientific, Singapore, 1989), p. 354.
- ⁵D. H. Ryan, J. M. D. Coey, E. Batalla, Z. Altounian, and J. O. Ström-Olsen, *Phys. Rev. B* **35**, 8630 (1987).
- ⁶H. Wakabayashi, K. Fukamichi, H. Komatsu, T. Goto, and K. Kuroda, in *Proceedings of The International Symposium on Physics of Magnetic Materials* (World Scientific, Singapore, 1987), p. 342.
- ⁷K. Fukamichi, T. Goto, and U. Mizutani, *IEEE Trans. Magn.* **MAG-23**, 3590 (1987).
- ⁸P. Hansen, in *Handbook of Magnetic Materials*, edited by K. H. J. Buschow (North-Holland, Amsterdam, 1991), Vol. 6, p. 289.
- ⁹J. Friedel, *Nuovo Cimento* **10**, Suppl. 2, 287 (1958).
- ¹⁰A. R. Williams, V. L. Moruzzi, A. P. Malozemoff, and K. Terakura, *IEEE Trans. Magn.* **MAG-19**, 1983 (1983).
- ¹¹A. P. Malozemoff, A. R. Williams, and V. L. Moruzzi, *Phys. Rev. B* **29**, 1620 (1984).
- ¹²M. Sostarich, *J. Appl. Phys.* **67**, 5793 (1990).
- ¹³A. P. Malozemoff, A. R. Williams, K. Terakura, V. L. Moruzzi, and K. Fukamichi, *J. Magn. Mater.* **35**, 192 (1983).
- ¹⁴T. Stobiecki, G. Beyreuther, and H. Hoffmann, in *Proceedings of Symposium on Magnetic Properties of Amorphous Metals* (Benalmadena, Spain, 1987); S. Krompiewski, U. Krauss, and U. Krey, *Phys. Rev. B* **39**, 2819 (1989).
- ¹⁵H. U. Krebs, W. Biegel, A. Bienenstock, D. J. Webb, and T. H. Geballe, *Mater. Sci. Eng.* **97**, 163 (1988).
- ¹⁶Y. Kakehashi, *Phys. Rev. B* **40**, 11 063 (1989).
- ¹⁷M. Cyrot, *J. Phys. (Paris)* **33**, 25 (1972).
- ¹⁸J. Hubbard, *Phys. Rev. B* **19**, 2626 (1979); **20**, 4584 (1979); **23**, 5974 (1981).
- ¹⁹H. Hasegawa, *J. Phys. Soc. Jpn.* **46**, 1504 (1979); **49**, 178 (1980).
- ²⁰P. Soven, *Phys. Rev.* **156**, 809 (1967); B. Velicky, S. Kirkpatrick, and H. Ehrenreich, *ibid.* **175**, 747 (1968).
- ²¹M. Yu and Y. Kakehashi, *J. Appl. Phys.* **73**, 3426 (1993).
- ²²Y. Kakehashi and H. Tanaka, *J. Magn. Magn. Mater.* **104-107**, 91 (1992).
- ²³Y. Kakehashi, H. Tanaka, and M. Yu, *Phys. Rev. B* **47**, 7736 (1993).
- ²⁴A. Arai, *J. Appl. Phys.* **64**, 3143 (1988).
- ²⁵Y. Kakehashi, *Phys. Rev. B* **41**, 9207 (1990).
- ²⁶Y. Kakehashi, *Phys. Rev. B* **43**, 10 820 (1991).
- ²⁷Y. Kakehashi, *Phys. Rev. B* **47**, 3185 (1993).
- ²⁸F. Matsubara, *Prog. Theor. Phys.* **52**, 1124 (1974).
- ²⁹S. Katsura, S. Fujiki, and S. Inawashiro, *J. Phys. C* **12**, 2839 (1979).
- ³⁰I. Turek, Ch. Becker, and J. Hafner, *J. Phys. Condens. Matter* **4**, 7257 (1992).
- ³¹S. Q. Wang, W. E. Evenson, and J. R. Schrieffer, *Phys. Rev. Lett.* **23**, 92 (1969); W. Evenson, J. R. Schrieffer, and S. Q. Wang, *J. Appl. Phys.* **41**, 1199 (1970).
- ³²Y. Kakehashi, *Phys. Rev. B* **34**, 3243 (1986).
- ³³For a review on the functional integral method see G. Morandi, E. Galleani, D'Agliano, and C. F. Ratto, *Adv. Phys.* **23**, 867 (1974); P. Fulde, *Electron Correlations in Molecules and*

- Solids*, Solid State Sciences Vol. 100 (Springer-Verlag, Berlin, 1991).
- ³⁴H. Shiba, *Prog. Theor. Phys.* **46**, 77 (1971).
- ³⁵V. Heine, *Phys. Rev.* **153**, 673 (1967).
- ³⁶U. K. Poulsen, J. Kollár, and O. K. Andersen, *J. Phys. F* **6**, L241 (1976).
- ³⁷A. Bieber and F. Gautier, *Solid State Commun.* **39**, 149 (1981); T. Oguchi, K. Terakura, and N. Hamada, *J. Phys. F* **13**, 145 (1983).
- ³⁸Y. Kakehashi, *Phys. Rev. B* **35**, 4973 (1987).
- ³⁹H. Miwa, *Prog. Theor. Phys.* **52**, 1 (1974).
- ⁴⁰Y. Kakehashi, *Prog. Theor. Phys.* **101**, 105 (1990).
- ⁴¹T. Fujiwara, *Nippon Butsuri Gakkaishi* **40**, 209 (1985).
- ⁴²J. F. Janak, *Phys. Rev. B* **16**, 255 (1977).
- ⁴³M. Matsuura, H. Wakabayashi, T. Goto, H. Komatsu, and K. Fukamichi, *J. Phys. Condens. Matter* **1**, 2077 (1989).
- ⁴⁴R. Yamamoto and M. Doyama, *J. Phys. F* **9**, 617 (1979).
- ⁴⁵I. Turek and J. Hafner, *Phys. Rev. B* **46**, 247 (1992).
- ⁴⁶H. Früchtl and U. Krey, *J. Magn. Magn. Mater.* **94**, L20 (1991).
- ⁴⁷T. Miyazaki, Y. Ando, and M. Takahashi, *J. Magn. Magn. Mater.* **60**, 219 (1986); **60**, 227 (1986); S. Ishio, K. Nushiro, and M. Takahashi, *J. Phys. F* **16**, 1093 (1986).
- ⁴⁸Y. Kakehashi, *Phys. Rev. B* **38**, 474 (1988).
- ⁴⁹Y. Kakehashi, *J. Magn. Magn. Mater.* **37**, 189 (1983).
- ⁵⁰M. Gabay and G. Toulouse, *Phys. Rev. Lett.* **47**, 201 (1981).
- ⁵¹J. R. Thomson, H. Guo, D. H. Ryan, M. J. Zuckermann, and M. Grant, *Phys. Rev. B* **45**, 3129 (1992).
- ⁵²H. Ren and D. H. Ryan, *Phys. Rev. B* **47**, 7919 (1993).
- ⁵³G. S. Cargill, III and F. Spaepen, *J. Non-Cryst. Solids* **43**, 91 (1981).